Check for updates

Received: 8 April 2024 | Revised: 7 June 2024 | Accepted: 11 June 2024

DOI: 10.1002/psc.3630

RESEARCH ARTICLE

Journal of PeptideScience WILEY

Au(I) complexes installed on a self-assembled peptide efficiently catalyze intramolecular cyclization reactions

Valentina Pirovano | Patrizia Brini | Elisa Brambilla | Maria Luisa Gelmi | Alessandra Romanelli

Dipartimento di Scienze Farmaceutiche, Università degli Studi di Milano, Milan, Italy

Correspondence
Valentina Pirovano and Alessandra Romanelli, Dipartimento di Scienze Farmaceutiche, Università degli Studi di Milano, via Venezian 21, 20133 Milan, Italy.
Email: valentina.pirovano@unimi.it and alessandra.romanelli@unimi.it

Self-assembled peptides are used for diverse applications in the biomedical and technological fields. The morphology and function of the assembled systems are dictated by the peptide sequence and length. In this work, a supramolecular catalyst was obtained upon self-assembly of the diphenylalanine peptide conjugated to a triphenylphosphine Au(I) complex in acetonitrile. The assembled molecules were characterized by spectroscopic techniques and by scanning electron microscopy. The activity of the catalyst was tested on two substrates in cyclization reactions. The morphology and the dimensions of the assembled systems vary depending on the presence of a carboxyl versus an amide C-terminal end. The catalyst efficiently promotes intramolecular cyclization reactions. Results obtained encourage the use of self-assembled peptides for the obtainment of new and efficient catalysts.

KEYWORDS
cyclization, gold, peptide, phosphine, self-assembly

1 | INTRODUCTION

Supramolecular systems obtained upon self-assembly of short amino-acidic sequences are widely explored, since the discovery of the smallest self-assembled peptide (diphenylalanine, FF) in the core recognition motif of the beta amyloid peptide.[1] X-ray diffraction studies demonstrated that stacking between aromatic rings and hydrogen bonds between the peptide chain concurs to determine the tubular structure and properties of such aggregates.[2] It is demonstrated that subtle changes to the chemical structure of the peptide or changes to the protocols employed to trigger the assembly may result in even drastic changes in the structure of the assembled molecules.[3,4] The ease with which these systems are obtained, due to the small size of the building blocks and robust synthetic protocols, strongly stimulated the research in this field. Applications of self-assembled systems based on small peptides range from electrochemical sensors to hydrogel scaffolds to support cell growth or small molecule controlled release to the production of superhydrophobic surfaces.[5–10] Moreover, self-assembled peptides can be exploited as catalysts.[11–14] One of the first examples of self-assembled peptide catalyst was reported by Guler and Stupp and refers to nanofibers formed by self-assembled peptide amphiphiles that catalyze the hydrolysis of 2,4-dinitro phenylacetate through a histidine residue.[12] The efficiency of the self-assembled system was related to the high density of catalytic sites exposed on the nanofiber surface. Tripeptides such as FFX (X = H, R) bearing histine or arginine residues were also demonstrated to be able to catalyze ester hydrolysis with high efficiency.[11] In other examples, the assembly of peptides is driven by metal complexation; in a recent paper, Dolan et al. report the formation of ordered chiral structures obtained upon complexation of Ir-Cp* to the dipeptide Pro-Leu and the ability of these ligands to promote enantioselective reduction of ketones.[13] Interestingly, enantioselectivity strongly depends on self-association of metal-peptide building blocks. In a different example, peptide nanofibers, obtained upon self-assembly of peptide bolaamphiphiles, were decorated with Pd nanoparticles and employed to catalyze C-C coupling reactions.[15] With an operationally similar but conceptually different approach, we envisioned the possibility to obtain self-assembled systems, composed of the aforementioned dipeptide FF connected through a linker to a phosphine working as Au(I) ligand, and to explore their ability to catalyze intramolecular cyclization reactions (Figure 1).[16,17]

© 2024 European Peptide Society and John Wiley & Sons Ltd.

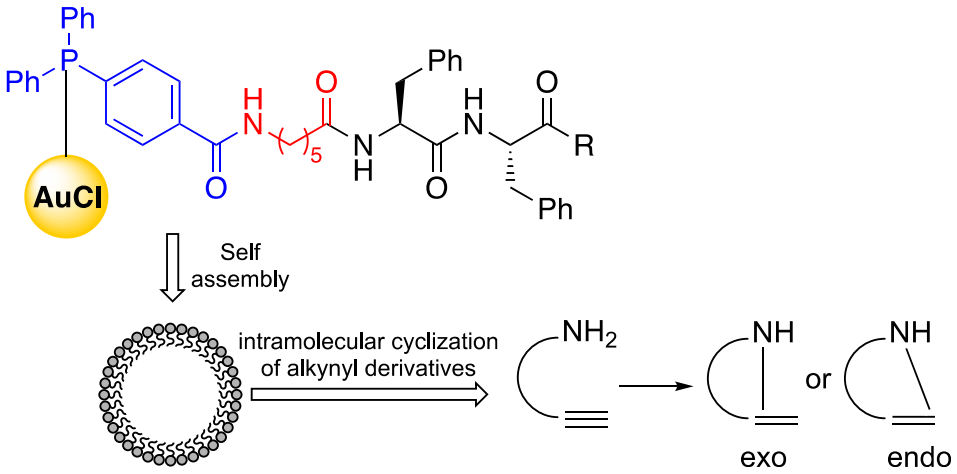

FIGURE 1 Aim of the work.

The metal is not coordinated to an amino-acid residue but to a ligand, covalently linked to the peptide. In particular, we chose linear 6-amino-hexanoic acid as linker between the N-terminus of the FF moiety and the carboxylic function of a triarylphosphine acting also as metal ligand. We chose 4-diphenylphosphine benzoic acid as ligand for the metal ion for two main reasons. First of all, triarylphosphines are among the simplest and more efficient ligands in gold catalysis displaying easily tunable electronic and steric properties. Moreover, the 4-diphenylphosphine benzoic acid is commercially available, and this fulfills the requirement to use simple and cheap substrates to assemble new catalytic systems. To the best of our knowledge, Au(I) catalysts bearing self-assembled peptides as ligands are not described in literature. The present work means to explore the ability of the dipeptide FF conjugated to a phosphine Au(I) complex to self-assemble and to catalyze intramolecular cyclization reactions. We envisioned that the combination of a well-defined gold/ligand system with the rigid structure of the self-assembled peptides offers a unique and unexplored environment for the substrate subjected to the catalytic reaction. Indeed, the possibility to modulate the properties of the catalytic system by changing the structure of the three components (ligand, linker, peptide) of the self-assembled system offers the chance to produce in a simple way different catalysts.

2 | MATERIALS AND METHODS

All chemicals and solvents are commercially available and were used as received. Silica gel F254 thin-layer plates were employed for thin-layer chromatography (TLC). Silica gel 40–63 μm/60 Å was employed for flash column chromatography. ^{1}H and ^{13}C and ^{31}P-NMR spectra were determined with a Varian-Gemini 300, a Bruker 300 Avance spectrometer at room temperature (rt) in $CDCl_3$, DMSO-d_6, or CD_2Cl_2 with residual solvent peaks as the internal reference. The attached proton test (APT) sequences were used to distinguish the methine and methyl carbon signals from those arising from methylene and quaternary carbon atoms. Low-resolution MS spectra were recorded with a Thermo-Finnigan LCQ advantage AP electrospray/ion trap equipped instrument using a syringe pump device to directly inject sample solutions.

Methyl (*tert*-butoxycarbonyl)phenylalanylphenylalaninate (**1**), 6-[(*tert*-butoxycarbonyl)amino]hexanoic acid (Boc-Ahx-OH), *N*-(prop-2-yn-1-yl)benzamide (**7**), and 2-(phenylethynyl)aniline (**9**) are known compounds and were prepared according to literature procedures.[18–21]

2.1 | Synthesis of Compounds 2–6

2.1.1 | Synthesis of methyl {6-[(*tert*-butoxycarbonyl)amino]hexanoyl}-L-phenylalanyl-L-phenylalaninate (**2**)

Methyl (*tert*-butoxycarbonyl)phenylalanylphenylalaninate (**1**) was dissolved in a CH_2Cl_2/trifluoro acetic acid (TFA) 80:20 v/v solution at a 0.07 M concentration. The reaction proceeded at rt for 1 h. The TFA was evaporated under reduced pressure and the product (H-FF-OMe) was precipitated with diethyl ether, isolated by centrifugation, and dried under vacuum (yield 97%). Subsequently, the compound was coupled with Boc-Ahx-OH. A solution of 6-[(*tert*-butoxycarbonyl)amino]hexanoic acid in CH_2Cl_2 (0.16 M) was cooled to 0°C and treated with 1-Ethyl-3-[3-dimethylaminopropyl]carbodiimide (EDC) (1.1 eq), 1-hydroxybenzotriazole (HOBT) (1.1 eq) and *N*,*N*-diisopropylethylamine (DIPEA) (2.7 eq). Subsequently, 0.9 eq of H-FF-OMe was added, and the reaction was stirred at rt for 16 h. The solvent was evaporated under reduced pressure. The residue was dissolved in ethyl acetate (EtOAc), a white solid precipitated: the solution was filtered and washed with HCl 1 M (×2) and brine. The product was purified by silica gel chromatography (CH_2Cl_2/EtOAc 3:1) to give methyl {6-[(*tert*-butoxycarbonyl)amino]hexanoyl}-L-phenylalanyl-L-phenylalaninate (**2**) with a final yield of 71%.

2.1.2 | Synthesis of methyl {6-[4-(diphenylphosphaneyl)benzamido]hexanoyl}-L-phenylalanyl-L-phenylalaninate (**3**)

Methyl {6-[(*tert*-butoxycarbonyl)amino]hexanoyl}-L-phenylalanyl-L-phenylalaninate (**2**) was dissolved in a CH_2Cl_2/TFA 80/20 v/v solution

10991387, 0, Downloaded from https://onlinelibrary.wiley.com/doi/10.1002/psc.3630 by UniversitaDegli Studi Di Mila, Wiley Online Library on [01/07/2024]. See the Terms and Conditions (https://onlinelibrary.wiley.com/terms-and-conditions) on Wiley Online Library for rules of use; OA articles are governed by the applicable Creative Commons License

at a 0.07 M concentration. The reaction proceeded at rt for 1 h. The TFA was evaporated under reduced pressure, and the product was precipitated with diethyl ether, isolated by centrifugation, and dried under vacuum (yield 99%). The resulting compound with a free amine was dissolved in CH_2Cl_2 at 0.1 M concentration and treated with 4-diphenylphoshanil benzoic acid (1 eq) in the presence of HOBT (1 eq), 2-(1*H*-benzotriazole-1-yl)-1,1,3,3-tetramethyluronium hexafluorophosphate (HBTU) (1 eq), and DIPEA (3 eq). After 16 h at rt, the solvent was evaporated under reduced pressure, and the residue was diluted with ethyl acetate and water. Phases were separated, and the organic layer was washed with $NaHCO_3$ saturated solution (s.s.), citric acid (10%), brine dried over Na_2SO_4, and concentrated under vacuum. The crude was purified by silica gel chromatography (CH_2Cl_2/MeOH 98:2) to give methyl {6-[4-(diphenylphosphaneyl)benzamido]hexanoyl}-L-phenylalanyl-L-phenylalaninate (**3**) as a white solid with a final yield of 87%.

2.1.3 | Synthesis of {6-[4-(diphenylphosphaneyl) benzamido]hexanoyl}-L-phenylalanyl-L-phenylalanine (**4**)

Methyl {6-[4-(diphenylphosphaneyl)benzamido]hexanoyl]-L-phenylalanyl-L-phenylalaninate (**3**) was dissolved in tetrahydrofuran (THF) at 0.1 M concentration and cooled down to 0°C; then 1.4 eq of $LiOH{\cdot}H_2O$ dissolved in water (0.25 M) was added. After stirring for 1 h, the solution was acidified up to pH 3 upon the addition of HCl 1 M. The crude was extracted with EtOAc (3×), the organic layer was dried over Na_2SO_4, and the solvent was evaporated under vacuum. The crude was purified by silica gel chromatography (CH_2C_{l2}/MeOH 95:5 + 0.1% formic acid) to give {6-[4-(diphenylphosphaneyl)benzamido]hexanoyl}-L-phenylalanyl-L-phenylalanine (**4**) as a white solid in 89% yield.

2.1.4 | Synthesis of methyl {6-[4-(diphenylphosphaneyl)benzamido]hexanoyl}-L-phenylalanyl-L-phenylalaninate gold(I) chloride (**5**)

{6-[4-(Diphenylphosphaneyl)benzamido]hexanoyl}-L-phenylalanyl-L-phenylalaninate (**3**) was dissolved in CH_2Cl_2 at 0.1 M concentration, dimethylsulfide chloride Au(I) (1.0 eq) was added under N_2, and the solution was stirred for 1 h at rt. The solvent was evaporated under reduced pressure to give an oily residue. Trituration with cold pentane gave **5** as a white solid in 94% yield.

2.1.5 | Synthesis of {6-[4-(diphenylphosphaneyl) benzamido]hexanoyl}-L-phenylalanyl-L-phenylalanine gold(I) chloride (**6**)

{6-[4-(Diphenylphosphaneyl)benzamido]hexanoyl}-L-phenylalanyl-L-phenylalanine (**4**) was dissolved in CH_2Cl_2 at 0.1 M concentration, dimethylsulfide chloride Au(I) (1.0 eq) was added under N_2, and the solution was stirred for 1 h at rt. The solvent was evaporated under reduced pressure to give an oily residue. Trituration with cold pentane gave **6** as a white solid in 95% yield.

2.2 | General procedure for catalytic reactions

To a nitrogen-flushed solution of catalysts **5** or **6** (5 mol%) in CH_3CN (0.1 M), $(CF_3SO_3)Ag$ or $AgSbF_6$ (5 mol%) was added, and the mixture was stirred for 5 min at rt. Then, *N*-(prop-2-yn-1-yl)benzamide (**7**) or 2-(phenylethynyl)aniline (**9**) was added, and the reaction was stirred until completion (monitored by TLC). The solvent was removed under vacuum, and the crude was purified by silica gel chromatography (hexane/EtOAc 95:5) to yield the corresponding products **8** and **10**.

2.3 | Circular dichroism (CD)

Analyses were performed on Jasco J810 instrument using a 0.1 mm quartz cuvette. Samples were dissolved in CH_3CN at 10 mg/mL, diluted to 3 mg/mL, and analyzed in the 275–208 nm wavelength range. Analyses of the samples at wavelengths higher than 275 nm revealed the absence of signals. Spectra were acquired using the following parameters: scan speed: 50 nm/min, bandwidth: 1 nm, and three accumulations.

2.4 | Fluorescence

Analyses were performed on a Perkin Elmer LS50B or a Fluorolog Jobin Yvon Horiba instrument at 25°C in CH_3CN. Excitation wavelength was set at 320 nm and emission wavelength at 440 nm. Samples dissolved in DMSO at 100 mg/mL were diluted to 2 mg/mL in CH_3CN to record excitation and emission spectra. Spectra obtained by dissolving samples directly in CH_3CN at the desired concentration were identical to those obtained upon dilution of DMSO solutions. Emission spectra were also recorded on samples obtained by serial dilution up to 0.25 mg/mL concentration (Figure S1).

2.5 | Scanning electron microscopy

Analyses were performed on a SEM-EDS JSM-IT500 LV from JEOL Spa (Italy). Samples were dissolved in CH_3CN at 10 mg/mL concentration; one drop of each sample was dried on an aluminum stub, using carbon tab covered with a glass slide. Samples were sputter-coated with a thin layer of gold using a Scancoat six sputter coater Edwards (1996). Images were acquired in high vacuum, using an acceleration tension of 20 kV, a 2.51 μA load current, and a 40 μA beam current.

10991387, 0, Downloaded from https://onlinelibrary.wiley.com/doi/10.1002/psc.3630 by UniversitaDegli Studi Di Mila, Wiley Online Library on [01/07/2024]. See the Terms and Conditions (https://onlinelibrary.wiley.com/terms-and-conditions) on Wiley Online Library for rules of use; OA articles are governed by the applicable Creative Commons License

3 | RESULTS AND DISCUSSION

In the first part of our studies, we realized the synthesis of two new gold(I) complexes, Compounds **5** (Au-FF-OMe) and **6** (Au-FF-OH) (Scheme 1) from ready-available precursors. A first coupling between *N*-Boc phenylalanine and phenylalanine methyl ester afforded methyl (*tert*-butoxycarbonyl)-L-phenylalanyl-L-phenylalaninate (**1**) in 71% yield.[15] Then, FF derivative **1** was deprotected at the N-terminus and coupled with 6-[(*tert*-butoxycarbonyl)amino]hexanoic acid to give **2**, in which the FF residue was connected to a six carbon unit linker, with overall yield for the two steps of 90%. This derivative was then coupled with commercially available 4-diphenylphosphine benzoic acid yielding FF-phosphine **3** in excellent 87% yield.[18,22] Finally, the corresponding gold(I) Complex **5** was obtained in 94% yield by reacting **3** with gold(I) chloride dimethyl sulfide complex. Alternatively, FF-phosphine **3** could be also deprotected at the methyl ester terminus with LiOH in THF/H_2O to give **4**, which, after reaction with gold(I) chloride dimethyl sulfide complex, afforded Complex **6** in 95% yield.[23] The identity and purity of isolated Complexes **5** and **6** and of all synthetized compounds were determined via nuclear magnetic resonance (NMR) studies (see Supporting information for details).

The conceivable self-assembly of synthetized systems **5** and **6** in solution was analyzed by spectroscopic studies, namely, fluorescence and CD. Fluorescence studies are suitable to study self-assembly of proteins, peptides, and hybrid molecules.[24–27] In particular, the appearance of intrinsic fluorescence signals suggests the formation in solution of self-assembled structures in which electron delocalization is responsible for the onset of the fluorescence phenomenon. These signals have been observed in protein fibrils as well as in FF and other dipeptides conjugated to PEG or other moieties; the appearance of fluorescence signals around 440 nm was observed in Fmoc-FF or Fmoc-GF and was attributed to aromatic groups stacked through π-π interactions.[28,29] Fluorescence measurements were performed on Au-FF-OMe (**5**) and Au-FF-OH (**6**) at different concentrations in CH_3CN and CH_2Cl_2. Fluorescence signals were detected only for samples prepared in CH_3CN (Figure 2). The lack of signals in CH_2Cl_2 was attributed to the lack of aggregation in this condition. For both complexes, we observe a maximum in the excitation spectrum around 320 nm and a maximum in the emission spectrum around 440 nm; in all cases, the intensity of the signal is concentration dependent. The fluorescence signal at 440 nm disappears at very low concentrations, when reasonably the aggregation does not occur. Control experiments run on the metal complex reveal the lack of signals at 440 nm (Figure S1). We can therefore conclude that the appearance of fluorescence signal at 440 nm is due to the formation of an organized structure in CH_3CN stabilized by stacking of aromatic rings, and on the basis of above reported literature evidences, we hypothesize that the dipeptide FF drives self-assembling. The presence of fluorescence signals of aggregates at concentration of 0.25 mg/mL (Figure S2) suggests that the critical aggregation concentration is lower than 0.25 mg/mL. Fluorescence experiments carried out incubating the aggregated compounds with the dye Congo Red, further support the aggregation phenomena. The fluorescence emission of the dye increases in the presence of beta sheets in aqueous buffer. As the experiments are carried out in CH_3CN, we cannot draw conclusions on the stabilization of the aggregates by beta sheet structures (Figure S3). CD studies are employed to determine the secondary structures of biological molecules including peptides and proteins and also for monitoring their self-assembly.[30–33] CD spectra of self-assembled peptides composed of polyphenylalanine or hybrid systems typically show signals between 200 and 230 nm, due to stacking between the aromatic amino acids and to hydrogen bonds between the backbone of different peptides that form beta sheet structures.[31,34] CD spectra were recorded on samples dissolved in CH_3CN (Figure 2C). Spectra of both samples show a maximum around 220 nm that is usually attributed to n-π* transitions due to aromatic stacking interactions between the phenylalanine side chains and a minimum around 238 nm.[35] This signal could be due to phosphines, as they show a maximum in the absorbance around 240 nm. Signals around 215 nm cannot be easily interpreted.

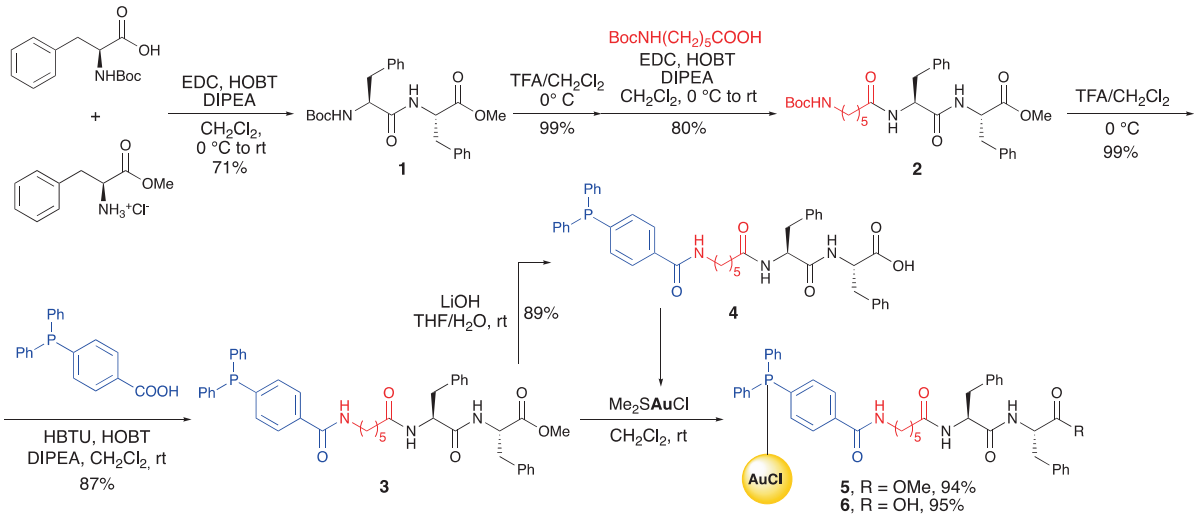

SCHEME 1 Synthesis of Complexes **5** and **6**.

10991387, 0, Downloaded from https://onlinelibrary.wiley.com/doi/10.1002/psc.3630 by UniversitaDegli Studi Di Mila, Wiley Online Library on [01/07/2024]. See the Terms and Conditions (https://onlinelibrary.wiley.com/terms-and-conditions) on Wiley Online Library for rules of use; OA articles are governed by the applicable Creative Commons License

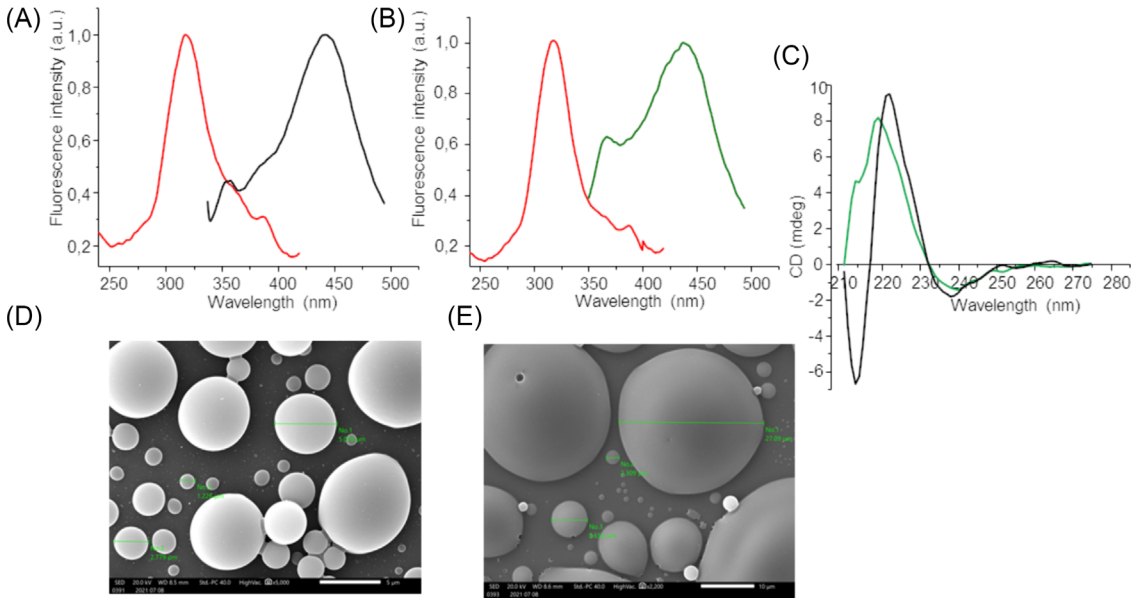

FIGURE 2 Fluorescence spectra of Au-FF-OH (A) and of Au-FF-OMe (B) in CH_3CN ($\lambda_{ex} = 320$ nm; $\lambda_{em} = 440$ nm). Excitation spectra are in red, emission spectra are in black and green. (C) Circular dichroism (CD) spectra of Au-FF-OMe (green) and Au-FF-OH (black) in CH_3CN. (D, E) SEM images of Au-FF-OH and Au-FF-OMe, respectively. Scale bar is 5 μM in (D) and 10 μM in (E).

TABLE 1 Preliminary catalytic trials.

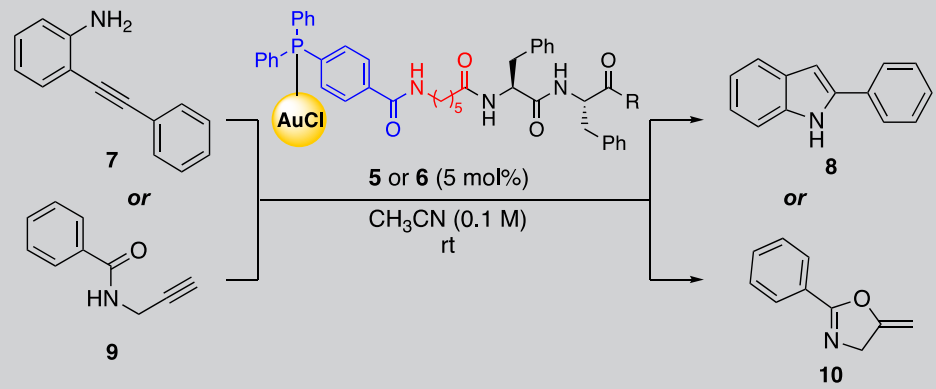

Entry	Substrate	[Au]	Additives	Time, h	Product, (%)[a]
1	**7**	5	-	48	n.r.[b]
2	**7**	6	-	48	n.r.[b]
3	**7**	5	$AgSbF_6$ (5 mol%)	48	8 (80%)
4	**7**	6	$AgSbF_6$ (5 mol%)	48	8 (82%)
5	**9**	5	$(CF_3SO_3)Ag$ (5 mol%)	2	10 (94%)
6	**9**	6	$(CF_3SO_3)Ag$ (5 mol%)	2	10 (88%)

Note: Reactions were performed with **7** or **9** (0.2 mmol), gold complex (5 mol%), and silver salt (0–5 mol%) in dry CH_3CN (2 mL, 0.1 M) at room temperature (rt).
[a]Isolated yield.
[b]Unreacted starting material was recovered at the end of the reaction.

Altogether, CD data indicate that self-assembly is triggered by stacking between phenylalanines in both cases; fluorescence results support this hypothesis. Finally, the morphology of the aggregates was determined by scanning electron microscopy. Images reported in Figure 2D,E show that Au-FF-OMe **5** forms irregularly shaped objects (vesicle-like), the most abundant with a diameter of 27 μm, whereas

10991387, 0, Downloaded from https://onlinelibrary.wiley.com/doi/10.1002/psc.3630 by UniversitaDegli Studi Di Mila, Wiley Online Library on [01/07/2024]. See the Terms and Conditions (https://onlinelibrary.wiley.com/terms-and-conditions) on Wiley Online Library for rules of use; OA articles are governed by the applicable Creative Commons License

Au-FF-OH **6** forms spherical aggregates; diameter of the spheres ranges from 1.2 to about 5 μm, with the most abundant being the smaller ones. The greater hydrophobicity of Compound **5** could be the reason of an "uncontrolled" aggregation that leads to the formation of objects with a greater dimension.

As a preliminary study on the catalytic activity of assembled Complexes **5** and **6**, we tested intramolecular hydroamination reaction of *ortho*-alkynylaniline **7** for the synthesis of indole **8** and the cyclization of *N*-propargylcarboxy amide **9** to give dihydrooxazole **10** (Table 1).[20,36] In both cases, we selected a catalyst loading of 5 mol% in 2 mL of CH_3CN (0.1 M referred to **7** or **9**), the catalyst concentration is higher than the estimated critical aggregation concentration. At first, *ortho*-alkynylaniline **7** was reacted in the presence of 5 mol% of catalysts; however, even after 48 h, any product was formed and we could recover unreacted **7**. On the other hand, the generation of the corresponding cationic gold(I) species by chloride abstraction with $AgSbF_6$ led to the formation of 2-phenylindole **8** in high yields with both catalysts **5** and **6**. Similar conditions were then applied to the cyclization of *N*-propargylcarboxy amides **9**. Also in this case, after 2 h, we were able to isolate dihydrooxazole **10** in 94% and 88% yields. These results, although preliminary, indicate a similar catalytic activity for both complexes Au-FF-OMe **5** and Au-FF-OH **6**. Deeper investigations on other substrates are ongoing in our laboratory to verify alternative reaction pathways and possible different stereoselectivities dictated by the supramolecular aggregation.[37]

4 | CONCLUSIONS

In conclusion, we demonstrated that Complexes **5** and **6** self-assemble to give microscopic structures stabilized by stacking between phenylalanine side chains. The supramolecular catalyst efficiently promotes intramolecular cyclization reactions. The difference in the CD spectra of self-assembled **5** and **6**, as well as the difference in the dimensions of the spheroids, suggests a different arrangement of **5** and **6** that could be due to a difference in the hydrophobicity, resulting in uncontrolled and disordered growth of aggregates in the case of **6** and in more regular structures in Compound **5**. The concentration of available catalytic units seems to be comparable in the two aggregates, being the cyclization reaction yields comparable. The finding that the synthetized supramolecular catalysts are active in promoting intramolecular cyclization reactions poses the bases for further investigations aimed at developing more efficient compounds.

ORCID

Alessandra Romanelli https://orcid.org/0000-0002-7609-4061

REFERENCES

1. Reches M, Gazit E. Casting metal nanowires within discrete self-assembled peptide nanotubes. *Science*. 2003;300(5619):625-627. doi:10.1126/science.1082387
2. Gorbitz CH. The structure of nanotubes formed by diphenylalanine, the core recognition motif of Alzheimer's beta-amyloid polypeptide. *Chem Commun (Camb)*. 2006;22(22):2332-2334. doi:10.1039/B603080G
3. Mason TO, Chirgadze DY, Levin A, et al. Expanding the solvent chemical space for self-assembly of dipeptide nanostructures. *ACS Nano*. 2014;8(2):1243-1253. doi:10.1021/nn404237f
4. Li Q, Jia Y, Dai LR, Yang Y, Li JB. Controlled rod nanostructured assembly of diphenylalanine and their optical waveguide properties. *ACS Nano*. 2015;9(3):2689-2695. doi:10.1021/acsnano.5b00623
5. Abbas M, Zou Q, Li S, Yan X. Self-assembled peptide- and protein-based nanomaterials for antitumor photodynamic and photothermal therapy. *Adv Mater*. 2017;29(12):1605021. doi:10.1002/adma.201605021
6. Sis MJ, Webber MJ. Drug delivery with designed peptide assemblies. *Trends Pharmacol Sci*. 2019;40(10):747-762. doi:10.1016/j.tips.2019.08.003
7. Matson JB, Stupp SI. Self-assembling peptide scaffolds for regenerative medicine. *Chem Commun*. 2012;48(1):26-33. doi:10.1039/C1CC15551B
8. Lee JS, Ryu J, Park CB. Bio-inspired fabrication of superhydrophobic surfaces through peptide self-assembly. *Soft Matter*. 2009;5(14):2717-2720. doi:10.1039/b906783c
9. Adler-Abramovich L, Badihi-Mossberg M, Gazit E, Rishpon J. Characterization of peptide-nanostructure-modified electrodes and their application for ultrasensitive environmental monitoring. *Small*. 2010;6(7):825-831. doi:10.1002/smll.200902186
10. Forlano N, Bucci R, Contini A, et al. Non-conventional peptide self-assembly into a conductive supramolecular rope. *Nanomaterials (Basel)*. 2023;13(2):333. doi:10.3390/nano13020333
11. Huang ZP, Guan SW, Wang YG, et al. Self-assembly of amphiphilic peptides into bio-functionalized nanotubes: a novel hydrolase model. *J Mater Chem B*. 2013;1(17):2297-2304. doi:10.1039/c3tb20156b
12. Guler MO, Stupp SI. A self-assembled nanofiber catalyst for ester hydrolysis. *J Am Chem Soc*. 2007;129(40):12082-12083. doi:10.1021/ja075044n
13. Dolan MA, Basa PN, Zozulia O, et al. Catalytic nanoassemblies formed by short peptides promote highly enantioselective transfer hydrogenation. *ACS Nano*. 2019;13(8):9292-9297. doi:10.1021/acsnano.9b03880
14. Zozulia O, Dolan MA, Korendovych IV. Catalytic peptide assemblies. *Chem Soc Rev*. 2018;47(10):3621-3639. doi:10.1039/C8CS00080H
15. Maity I, Rasale DB, Das AK. Peptide nanofibers decorated with Pd nanoparticles to enhance the catalytic activity for C-C coupling reactions in aerobic conditions. *RSC Adv*. 2014;4(6):2984-2988. doi:10.1039/C3RA44787A
16. Hashmi ASK. Gold-catalyzed organic reactions. *Chem Rev*. 2007;107(7):3180-3211. doi:10.1021/cr000436x
17. Lu ZC, Hammond GB, Xu B. Improving homogeneous cationic gold catalysis through a mechanism-based approach. *Acc Chem Res*. 2019;52(5):1275-1288. doi:10.1021/acs.accounts.8b00544
18. Maity S, Nir S, Zada T, Reches M. Self-assembly of a tripeptide into a functional coating that resists fouling. *Chem Commun*. 2014;50(76):11154-11157. doi:10.1039/C4CC03578J
19. Biraboneye AC, Madonna S, Laras Y, Krantic S, Maher P, Kraus JL. Potential neuroprotective drugs in cerebral ischemia: new saturated and polyunsaturated lipids coupled to hydrophilic moieties: synthesis and biological activity. *J Med Chem*. 2009;52(14):4358-4369. doi:10.1021/jm900227u
20. Hashmi ASK, Weyrauch JP, Frey W, Bats JW. Gold catalysis: mild conditions for the synthesis of oxazoles from N-propargylcarboxamides and mechanistic aspects. *Org Lett*. 2004;6(23):4391-4394. doi:10.1021/ol0480067
21. Koradin C, Dohle W, Rodriguez AL, Schmid B, Knochel P. Synthesis of polyfunctional indoles and related heterocycles mediated by cesium and potassium bases. *Tetrahedron*. 2003;59(9):1571-1587. doi:10.1016/S0040-4020(03)00073-5

10991387, 0, Downloaded from https://onlinelibrary.wiley.com/doi/10.1002/psc.3630 by UniversitaDegli Studi Di Mila, Wiley Online Library on [01/07/2024]. See the Terms and Conditions (https://onlinelibrary.wiley.com/terms-and-conditions) on Wiley Online Library for rules of use; OA articles are governed by the applicable Creative Commons License

22. Kokan Z, Peric B, Kovacevic G, Brozovic A, Metzler-Nolte N, Kirin SI. Cis-versus trans-square-planar palladium(II) and platinum(II) complexes with triphenylphosphine amino acid bioconjugates. *Eur J Inorg Chem*. 2017;33(33):3928-3937. doi:10.1002/ejic.201700679
23. Kokan Z, Glasovac Z, Elenkov MM, Gredicak M, Jeric I, Kirin SI. "Backdoor induction" of chirality: asymmetric hydrogenation with rhodium(I) complexes of triphenylphosphane-substituted beta-turn mimetics. *Organometallics*. 2014;33(15):4005-4015. doi:10.1021/om5005385
24. Chan FT, Kaminski Schierle GS, Kumita JR, Bertoncini CW, Dobson CM, Kaminski CF. Protein amyloids develop an intrinsic fluorescence signature during aggregation. *Analyst*. 2013;138(7):2156-2162. doi:10.1039/c3an36798c
25. Pinotsi D, Buell AK, Dobson CM, Kaminski Schierle GS, Kaminski CF. A label-free, quantitative assay of amyloid fibril growth based on intrinsic fluorescence. *ChemBioChem*. 2013;14(7):846-850. doi:10.1002/cbic.201300103
26. Handelman A, Kuritz N, Natan A, Rosenman G. Reconstructive phase transition in ultrashort peptide nanostructures and induced visible photoluminescence. *Langmuir*. 2016;32(12):2847-2862. doi:10.1021/acs.langmuir.5b02784
27. Diaferia C, Avitabile C, Leone M, et al. Diphenylalanine motif drives self-assembling in hybrid PNA-peptide conjugates. *Chemistry*. 2021;27(57):14307-14316. doi:10.1002/chem.202102481
28. Tang C, Ulijn RV, Saiani A. Effect of glycine substitution on Fmoc-diphenylalanine self-assembly and gelation properties. *Langmuir*. 2011;27(23):14438-14449. doi:10.1021/la202113j
29. Smith AM, Williams RJ, Tang C, et al. Fmoc-diphenylalanine self assembles to a hydrogel via a novel architecture based on π-π interlocked β-sheets. *Adv Mater*. 2008;20(1):37-41. doi:10.1002/adma.200701221
30. Ranjbar B, Gill P. Circular dichroism techniques: biomolecular and nanostructural analyses—a review. *Chem Biol Drug Des*. 2009;74(2):101-120. doi:10.1111/j.1747-0285.2009.00847.x
31. Avitabile C, Diaferia C, Roviello V, et al. Fluorescence and morphology of self-assembled nucleobases and their diphenylalanine hybrid aggregates. *Chemistry*. 2019;25(65):14850-14857. doi:10.1002/chem.201902709
32. Mosseri A, Sancho-Albero M, Leone M, et al. Chiral fibers formation upon assembly of tetraphenylalanine peptide conjugated to a PNA dimer. *Chem - Eur J*. 2022;28(37):e202200693. doi:10.1002/chem.202200693
33. Mosseri A, Sancho-Albero M, Mercurio FA, Leone M, De Cola L, Romanelli A. Tryptophan-PNA gc conjugates self-assemble to form fibers. *Bioconjug Chem*. 2023;34(8):1429-1438. doi:10.1021/acs.bioconjchem.3c00200
34. Adler-Abramovich L, Reches M, Sedman VL, Allen S, Tendler SJB, Gazit E. Thermal and chemical stability of diphenylalanine peptide nanotubes: implications for nanotechnological applications. *Langmuir*. 2006;22(3):1313-1320. doi:10.1021/la052409d
35. Castelletto V, Hamley IW. Self assembly of a model amphiphilic phenylalanine peptide/polyethylene glycol block copolymer in aqueous solution. *Biophys Chem*. 2009;141(2–3):169-174. doi:10.1016/j.bpc.2009.01.008
36. Arcadi A, Bianchi G, Marinelli F. Gold(III)-catalyzed annulation of 2-alkynylanilines: a mild and efficient synthesis of indoles and 3-haloindoles. *Synthesis (Stuttgart)*. 2004;4(4):610-618. doi:10.1055/s-2004-815947
37. Jans ACH, Caumes X, Reek JNH. Gold catalysis in (supra)molecular cages to control reactivity and selectivity. *ChemCatChem*. 2018;11(1):287-297. doi:10.1002/cctc.201801399

SUPPORTING INFORMATION

Additional supporting information can be found online in the Supporting Information section at the end of this article.

How to cite this article: Pirovano V, Brini P, Brambilla E, Gelmi ML, Romanelli A. Au(I) complexes installed on a self-assembled peptide efficiently catalyze intramolecular cyclization reactions. *J Pept Sci*. 2024;e3630. doi:10.1002/psc.3630

10991387, 0, Downloaded from https://onlinelibrary.wiley.com/doi/10.1002/psc.3630 by UniversitaDegli Studi Di Mila, Wiley Online Library on [01/07/2024]. See the Terms and Conditions (https://onlinelibrary.wiley.com/terms-and-conditions) on Wiley Online Library for rules of use; OA articles are governed by the applicable Creative Commons License